www.czasopisma.pan.pl PAN POLSKA AKADEMIA NAUK www.journals.pan.pl

A R C H I V E S O F M E T A L L U R G Y A N D M A T E R I A L S

Volume 59 2014 Issue 2

DOI: 10.2478/amm-2014-0081

D. KALISZ*

INTERACTION OF NON-METALLIC INCLUSION PARTICLES WITH ADVANCING SOLIDIFICATION FRONT

ODDZIAŁYWANIE CZĄSTEK WYDZIELEŃ NIEMETALICZNYCH Z POSTĘPUJĄCYM FRONTEM KRZEPNIĘCIA

This work deals the phenomenon interaction of crystallization front on the particles of non-metallic precipitates. The behavior of a single particle in the vicinity of horizontal and vertical front was analyzed. The forces acting on the particle were characterized and the equilibrium condition formulated, from which the critical velocity of front may be deduced. The calculation results were illustrated in the form of graphs.

Keywords: solidification front, non-metallic inclusions, forces

Praca zajmuje się zjawiskiem oddziaływania przemieszczającego frontu krystalizacji na cząstki wydzieleń niemetalicznych. Analizowano zachowanie pojedynczej cząstki wydzielenia w pobliżu poziomego i pionowego frontu. Scharakteryzowano siły działające na cząstkę w pobliżu frontu i sformułowano warunek równowagi, z którego wynika szybkość krytyczna frontu. Wyniki obliczeń zilustrowano w postaci wykresów.

1. Introduction

In the solidification process the non-metallic inclusions may be either engulfed or repelled by the advancing solidification front. Consequently, they may be evenly dispersed in the material or accumulated in certain areas. If the crystallization front has a cellular or dendritic character, the particle may be present within the field of activity of two local fronts simultaneously. If it has not been already engulfed by any of them, it will be entrapped in the last portion of the solidifying steel, most frequently in the ingot axis. The interaction of a particle with the crystallization front can be directly observed only on the liquid steel surface [1-2]. Depending on the chemical composition of the inclusion, its behavior differs in relation to the mobile solidification front.

The simplest criterion deciding about the engulfment by solidification front is the so-called free energy of absorption ΔG_p, defined as interface energy difference σ_{p-s} and σ_{p-l}. The engulfment takes place when:

$$\Delta G_p = \sigma_{p-s} - \sigma_{p-l} \leqslant 0 \tag{1}$$

where:

σ_{p-s} – surface energy of particle/solid metal system [N/m],

σ_{p-l} – surface energy of particle/liquid metal system [N/m],

This dependence, as given by Omeny and Neumann [3] in the form of a thermodynamic condition, is applicable to all low advancement rates of the solidification front. Meeting condition (1) is sufficient for a particle to adhere to the crystallization front. At higher solidification rates the particles are engulfed even when the absorbed free energy exceeds zero. The bigger is the diameter of the inclusion the smaller is the boundary rate, at which engulfing takes place.

2. Single particle near vertically advancing crystallization front

The correct analysis of interaction of an inclusion and solidification front should account for equilibrium of forces acting on the particle. In the simplest case, a single particle is present in the vicinity of the crystallization front in a system where no convective flow of the liquid occurs [4]. If a flat crystallization front moves up vertically at a constant rate of V, the behavior of the particle results from the balance of forces acting on it:

– force due to gravity i.e. difference between buoyancy and weight (F_g [N])

$$F_g = \frac{4}{3} \cdot \pi \cdot r^3 (\rho_m - \rho_p) \cdot g \tag{2}$$

where:

ρ_m – density of metal (steel) [kg/m^3],

ρ_p – density of particle (inclusion) [kg/m^3],

g – gravitational acceleration [m/s^2],

r – radius of a non-metallic inclusion [m].

– repulsive force,

Repulsive force (F_r [N]) between a solid, spherical particle of radius r and surface s/l is a result of a difference of

* AGH UNIVERSITY OF SCIENCE AND TECHNOLOGY, FACULTY OF FOUNDRY ENGINEERING, AL. A. MICKIEWICZA 30, 30-059 KRAKÓW, POLAND

surface energies $\Delta\sigma_0$ [4], [5]. As the repulsive force acts on a small distance, the following is assumed:

$$\Delta\sigma_0 = \sigma_{p-s} - (\sigma_{p-l} + \sigma_{s-l}) \geqslant 0 \tag{3}$$

where:

σ_{s-l} – surface energy of the liquid metal/solid metal system [N/m].

The repulsive force acts on a distance d_0, which is of atom size order. The denotation d_0 refers to the flat solidification front. When the distance in bigger, $x > d_0$, then the share of the surface energy decreases

$$\Delta\sigma = \Delta\sigma_0 \cdot \left(\frac{d_0}{x}\right)^n \tag{4}$$

σ_0 – [N/m],

d_0 – distance [m].

where: n = 2 to 7; this results from the type of interaction, for van der Waals force n=7. Repulsive force acting on a particle of radius r equals to:

$$F_r = \pi \cdot r \cdot \Delta\sigma \tag{5}$$

For a location $x = d_0 + r$, $F_r = 0$, and for $x = d_0$, $F_r > 0$. By transformation of formula (4) and (5), on the assumption that $r >> d_0$, we obtain:

$$F_r = -\frac{\pi \cdot r \cdot \Delta\sigma_0}{n-1} \tag{6}$$

Pötschke and Rogge [6] identify the repulsive force as an interaction of Van der Waalsa type, which can be presented by the following dependence:

$$F_r = \frac{32}{3} \cdot A \cdot \frac{r^3 \cdot R^3 \cdot (d_0 + r + R)}{d_0^2 \cdot (d_0 + 2R)^2 \cdot (d_0 + 2r)^2 \cdot (d_0 + 2r + 2R)^2} \tag{7}$$

where:

A – Hamaker constant,

R – radius of curvature of solidification front [m],

r – radius of non-metallic inclusion [m].

Radius of curvature R of surface s/l is assumed to be positive when its convexity is directed towards the liquid. For a flat boundary s/l ($R \to \infty$):

$$F_r^x = \lim_{R\to\infty} F_r = \frac{2}{3} \cdot A \cdot \frac{r^3}{d_0^2 \cdot (d_0 + 2r)^2} \tag{8}$$

On this basis the Hamaker constant can be determined, provided that the least value of d_0 equals to the interatomic distance in the grid a_0.

$$A = 12\pi \cdot a_0^2 \cdot \Delta\sigma \tag{9}$$

- drag force (F_d [N]) – resistance of viscous stream is connected with the viscosity of fluid and its value for a general case is regulated by Stokes law.

$$F_d = 6\pi \cdot \mu \cdot V \cdot r \tag{10}$$

where:

μ – dynamic viscosity of liquid [kg/m·s],

V – rate of solidification front in a steady state [m/s].

For the reason of allowing the solidification front to move up vertically at a certain distance from a particle, fresh liquid has to be constantly supplied to the space between the particle and the front. The distribution of the flow rate of fluid between two approximately parallel surfaces is calculated from Navier-Stokes equation:

$$V_l(x) = \frac{x \cdot (h - x)}{2 \cdot \mu} \cdot \frac{dP}{dR_c} \tag{11}$$

where:

h – distance between a non-metallic inclusion and the vertical solidification front [m],

R_c – radius of analyzed fragment of surface s/l [m],

P – pressure.

Stream J of a liquid flowing through the lateral surface of a cylinder of radius R_c equals to:

$$J = \int_0^{h(R_c)} V_l(x) \cdot 2\pi \cdot R_c \cdot dx \tag{12}$$

J – stream.

The same amount is crystallized in a unit of time:

$$J = \pi \cdot R_c^2 \cdot V \tag{13}$$

The drag force (F_d) is proportional to pressure in equation (11):

$$dF_d = \pi \cdot R_c^2 \cdot dP \tag{14}$$

By comparing (12) and (13), and accounting for (11) and (14) we can calculate the drag force, which for a small distance between the particle and the front ($d_0 << r$) is given by the equation:

$$F_d = 6\pi \cdot \mu \cdot V \cdot \frac{r^2}{d_0} \tag{15}$$

3. Calculation of gravity force F_g, repulsive force F_r and drag force F_d

On the basis of above presented equations (2), (3) and (10), exemplary calculation of gravity force F_g, repulsive force F_r and drag force F_d were conducted for an Al_2O_3 particle in steel. The following data were assumed for the calculation: ρ_m – density of metal (steel) 7000 [kg/m^3], ρ_p – density of inclusion (Al_2O_3) 3990 [kg/m^3], r – radius of inclusion 0.00001 – 0.0001 [m], μ – dynamic viscosity of steel 0.06 [Pa·s], V – rate of solidification front: 5 μm/s, 10 μm/s, 15μm/s, n=2, 3, 4, 5, 6 or 7.

Two variants were considered:

Variant 1	Variant 2
σ_{s-l} – 0.5 [N/m]	σ_{s-l} – 1.0 [N/m]
σ_{p-l} – 0.5 [N/m]	σ_{p-l} – 0.3 [N/m]
σ_{p-s} – 1.5 N/m]	σ_{p-s} – 1.5 N/m]

The results of calculation of the gravity force F_g acting on a non-metallic (Al_2O_3) particle as a function of the particle's radius are presented in Fig. 1.

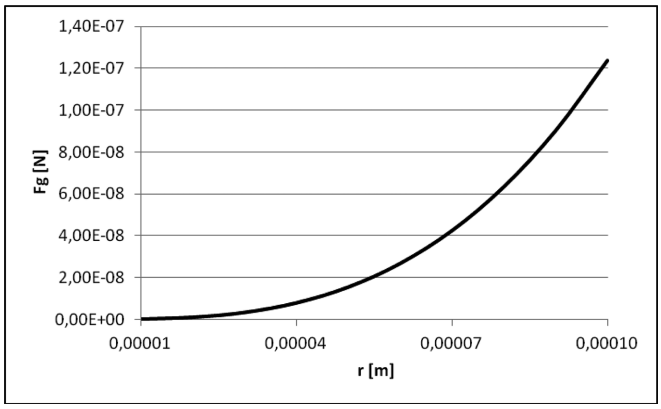

Fig. 1. Gravity force F_g against radius of inclusion (Al_2O_3) radius

The results of calculation of repulsive force F_r (6) between solid, spherical particle of radius r and surface s/l for: σ_{s-l} =0.5 [N/m], σ_{p-l} =0.5 [N/m], σ_{p-s} =1.5 [N/m] are presented in Fig. 2.

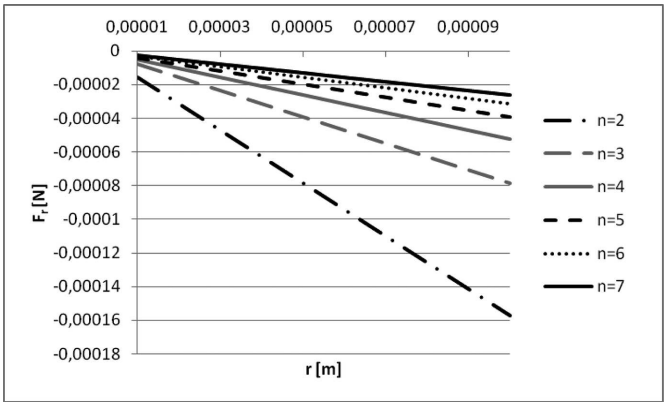

Fig. 2. Repulsive force F_r against radius of inclusion (Al_2O_3) for: σ_{s-l} – 0.5 [N/m], σ_{p-l} – 0.5 [N/m], σ_{p-s} – 1.5 [N/m]

The results of calculations of repulsive force F_r (6) acting on a spherical particle of aluminum oxide as a function of the radius of inclusion for: σ_{s-l} =1.0 [N/m], σ_{p-l} =0.3 [N/m], σ_{p-s} =1.5 [N/m] are presented in Fig. 3.

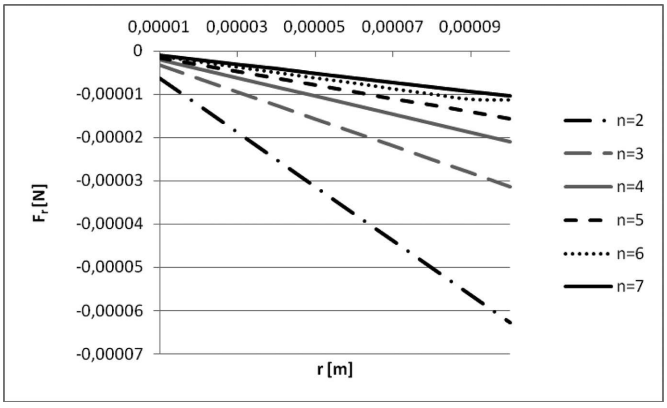

Fig. 3. Repulsive force F_r against radius of inclusion (Al_2O_3) for: σ_{s-l} – 1.0 [N/m], σ_{p-l} – 0.3 [N/m], σ_{p-s} – 1.5 [N/m]

The results of calculations of drag force F_d acting on a non-metallic particle disposed in a neighborhood of solidification front vertically moving at a rate of 5, 10 and 15 μm/s are presented in Fig. 4.

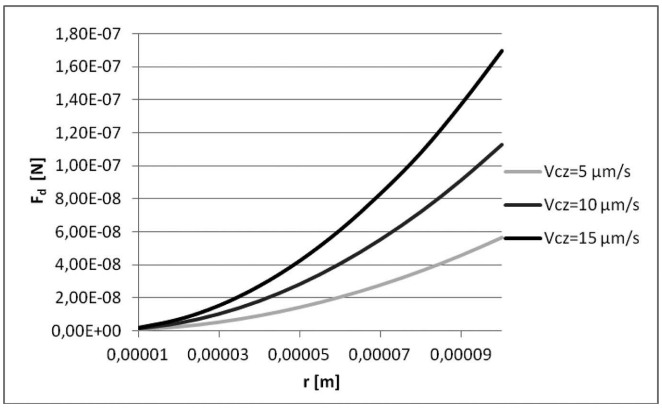

Fig. 4. Results of calculations of drag force F_d depending on the radius of Al_2O_3 particle in the vicinity of solidification front vertically moving at a rate of V=5 μm/s, 10 μm/s and 15 μm/s

The growth of a non-metallic (Al_2O_3) particle results in the increasing force of gravity F_g. Calculations conducted for the repulsive force F_d corresponding to the force acting on a particle (variants 1 and 2) indicate that the assumed coefficient n=2 (with the concurrent increase of the particle's size) causes a change of the repulsive force value by one order; for n=7 the difference of the repulsive force in variants 1 and 2 is over double, e.g. for a particle of a radius to 0.0001 m, the repulsive force equals to $-2.61 \cdot 10^{-5}$ and $-1.04 \cdot 10^{-5}$ in variants 1 and two, respectively (n=7).

4. Critical solidification rate

The rate at which the solidification front is advancing assumes a critical value V_{crit}, when the particle is in a stationary position in reference to the front, i.e. it is neither repelled nor attracted. In this state the forces acting on the particle can be assumed to be sustained:

$$\overline{F}_g + \overline{F}_r + \overline{F}_d = 0 \tag{16}$$

In the case of a non-metallic inclusion in liquid steel, the gravity force F_g is directed upwards, hence:

$$\overline{F}_g + \overline{F}_r = \overline{F}_d \tag{17}$$

After substituting expressions for particular forces from equations (2), (6) and (15) one can directly calculate the critical rate of solidification front movement. Having neglected the gravity force (for a small difference of density of particle and grid materials), Stefanescu et al. [7] gives a simplified dependence for the critical flow rate:

$$V_{crit} = \frac{\Delta\sigma_0 \cdot d_0}{6 \cdot (n-1) \cdot \mu \cdot r} \tag{18}$$

This dependence is not used for the metal/non-metallic inclusion system, when the density difference is high. When the rate of the front is lower than the critical value, the particles only are repelled, otherwise, they are absorbed. The analysis of equation (18) reveals that the critical solidification rate is higher for small-radius particles.

5. Single particle in the vicinity of a moving crystallization front

In the case of a vertical crystallization front which advances horizontally, the particle may be assumed to be immobile. The movement of the particle in reference to the front should be accounted for. The flat system of forces acting on the particle also covers the gravity force, expressed with the equation (2). The drag force of a viscous flow taking place in the opposite direction as compared to that of the particle, with the velocity V_p and in reference to fluid is presented in the following form [8]:

$$F_d = 6 \cdot \pi \cdot \mu \cdot r \cdot V_p \cdot \theta \tag{19}$$

where:

F_d – drag force of viscous flow,

μ – coefficient of dynamic viscosity [kg/m·s],

The value of coefficient θ depends on the flow direction of the particle and its distance from front h: $\theta = 1$ for a particle far away from the front, $\theta = \frac{r}{h}$ for a particle approaching the front, and $\theta = \ln\left(\frac{r}{h}\right)$ for a particle moving parallel to the front.

In the neighborhood of the solidification front the rate of the fluid's flow is non-homogeneous (component parallel to the front is important) and the concentration of liquid components is non-homogeneous (especially components of those low equilibrium partition coefficient $k^{s/l}$). A force due to the gradient of fluid velocity S, perpendicular to the front, in an area identified as a boundary velocity layer, can be treated as Saffman force [9]. Saffman force F_S [N] is defined by the following dependence:

$$F_s = 6,46 \cdot \mu \cdot r^2 \cdot V_p \cdot \sqrt{\frac{S}{v}} \tag{20}$$

where:

r – radius of inclusion [m],

v – kinematic viscosity [m^2/s],

S – local gradient of fluid velocity [m/s].

Force F_s may cause approaching or moving away of a particle from the front, depending on the direction of fluid's movement and a difference of particle and fluid densities. When the fluid is flowing down along the front and the density of the particle is higher than that of fluid, Saffman force moves away the particle from the front [9]. The non-homogeneity of concentration of a surface-active fluid component in the vicinity of the crystallization front (in the boundary concentration area) generates a force which brings the particle closer to the front surface (Marangoni effect). Mukai & Zeze [10] made an experiment for water solutions, where this effect occurred in the presence of a surfactant. Force F_M [N]acting on the particle is a function of gradient of interface energy σ_{p-l}:

$$F_M = -\frac{8}{3} \cdot \pi \cdot r^2 \cdot \frac{\partial \sigma_{p-l}}{\partial z} \tag{21}$$

where:

z – horizontal coordinate,

r – radius of an inclusion [μm].

Figure 5 shows equilibrium diagram of forces acting on a particle flowing down the vertical solidifying front.

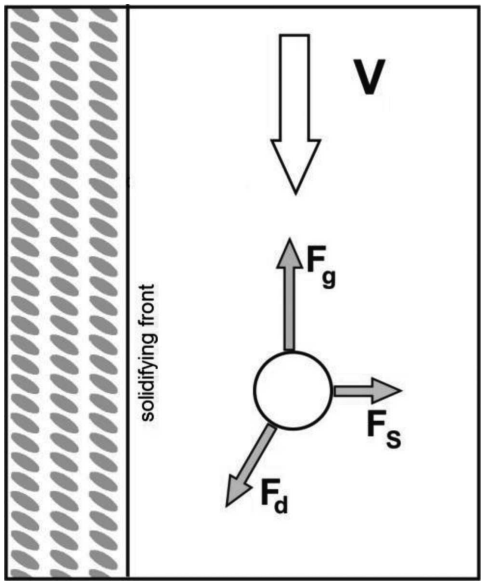

Fig. 5. Equilibrium of forces acting on a particle flowing down the vertical solidifying front [11]

The resultant velocity of the particle is also proportional to the gradient of interface energy. Experimental data on the critical value of solidification rate solely refer to particles on the surface of liquid metal with the crystallization front moving horizontally. As far as Al_2O_3 inclusions in steel are concerned, Shibata et al. [12] stated that the critical rate of the front can be expressed with the below dependence:

$$V_{crit} = \frac{60}{r} \quad (r\ w\ \mu m) \tag{22}$$

which gives 1.2 μm·$s^{-1}$for a particle of radius of 50 μm. Stefanescu et al. [7] observed that for SiC particles in low magnesium or nickel alloys of aluminum the values of V_{crit} are much higher for particles of radius equal to 50 μm, i.e. stay within a broad range of values from 8 to 400 μm·s^{-1}.

6. Exemplary calculation of frictional force F_d for a non-metallic particle in the vicinity of a vertical solidification front which is advancing horizontally

The frictional force F_d for a non-metallic particle in the vicinity of a vertical solidification front, which is advancing horizontally, was calculated on the basis of equation (19). The following assumptions were made:

μ – viscosity of steel 0.06 [Pa·s],

V_p – velocity of a non-metallic particle in respect to fluid: 5 μm/s, 10 μm/s, 15 μm/s.

Two variants were analyzed:

Variant 1: $\theta = 1$,

Variant 2: θ = r/h, dla h_1 = 0.000001[m],

h_2 = 0.00001[m].

The results of calculations are presented in Figures 6 to 8.

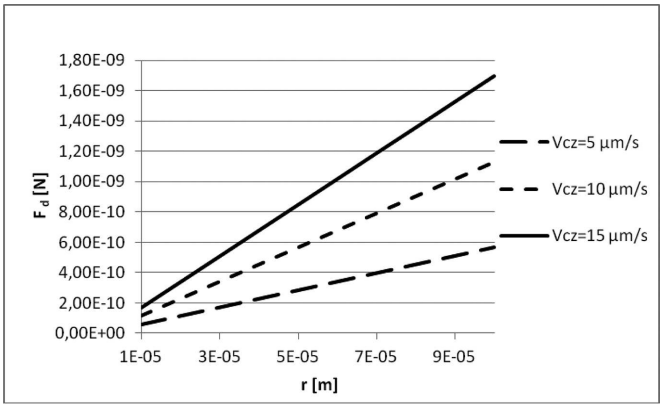

Fig. 6. Results of calculations of frictional force F_d for a non-metallic particle in the vicinity of a vertical solidification front which is advancing horizontally, for the particle velocities: 5 μm/s, 10 μm/s, 15 μm/s (variant 1)

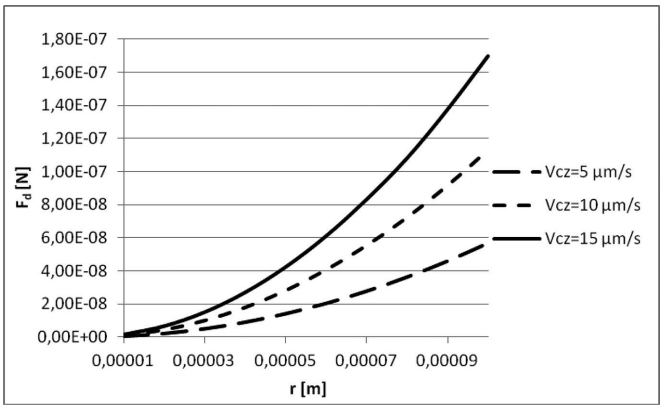

Fig. 7. Results of calculations of frictional force F_d for a non-metallic particle in the vicinity of a vertical solidification front which is advancing horizontally, for the particle velocities: 5 μm/s, 10 μm/s, 15 μm/s (variant 1), for h_1 = 0.000001 [m] (variant 2)

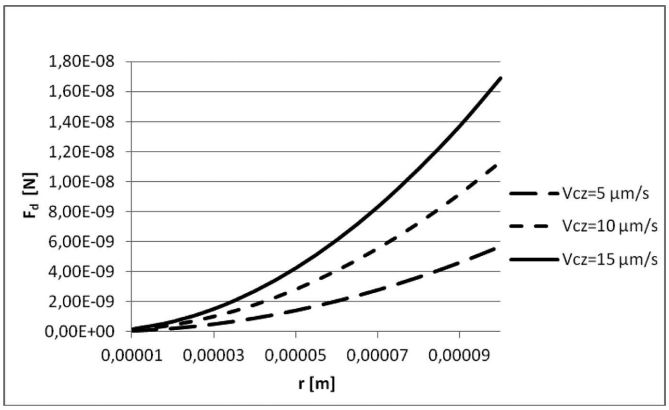

Fig. 8. Results of calculations of frictional force F_d for a non-metallic particle in the vicinity of a vertical solidification front which is advancing horizontally, for the particle velocities: 5 μm/s, 10 μm/s, 15 μm/s (variant 1), for h_2 = 0.00001 [m] (variant 2)

Calculations of the frictional force F_d for a non-metallic particle in the vicinity of a vertical front advancing horizontally for variants 1 and 2, determine the influence of radius of an inclusion on force F_d. The same increasing tendency of frictional force with the increasing velocity of the particle is maintained in all cases. In both variants the frictional force values increase with the increasing radius of the inclusion particle and with the velocity of the advancing solidification front. In variant 1 the frictional force was two orders lower than in variant 2 for h1 = 0.000001 [m] and one order lower than in calculations made for variant 2 for h1 = 0.00001 [m]. The frictional force mainly acts on particles in the close vicinity of the solidification front.

7. Morphology of particle engulfment

The engulfment of a particle, requiring exceeding of critical advancement rate of the front was presented in detail in Fig. 9. Here the field of temperature and field of forces acting on the particle, operate simultaneously. The equilibrium distance of a particle from the front can be determined for these fields individually. In the real process the moving particles and deformation of the solidification front cause that these two equilibrium distances become equal [13], [14] and [15].The relation between thermal conductivity of particle material k_p and the liquid metal k_m determines the shape of the crystallization front.

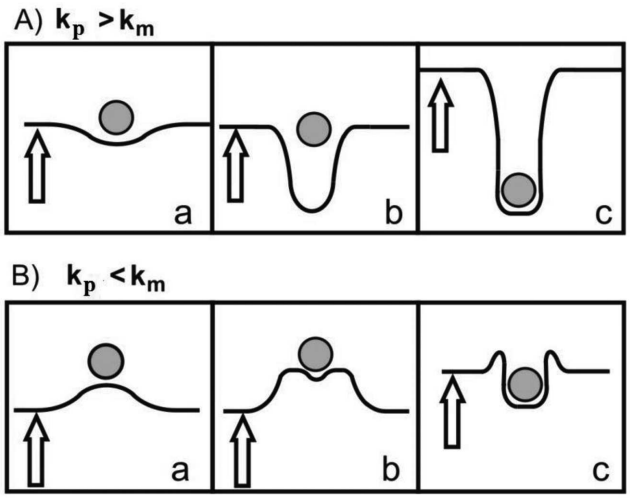

Fig. 9. Deformation of solidification front and engulfment of a particle for a front advancing faster than the critical velocity: A) for $k_p > k_m$, B) for $k_p < k_m$ [13,14,15]

For $k_p > k_m$ the engulfment begins with a concavity formed in the front, and for $k_p < k_m$ from a convexity formed in the front. Deformations of the solidification front may be considerable in size. For instance, Stefanescu at al. [4] made an experiment with small SiC particles in the solidifying dinitrile succinate. The obtained depth of concavity of front (Fig. 9.A.a) exceeded the particle's diameter over ten times.

8. The influence of fluid flow on engulfment of particles in the vertical continuous casting

Previous considerations were focused on the case in which the fluid does not flow along the horizontal solidification front. If this happens, the particle staying in contact with the crystallization front will roll on it. This movement is

generated by a force due to the fluid flow (its component is parallel to the crystallization front), and frictional force. The critical rate of flow of metal, above which the rolling takes place, can be calculated. The flow of fluid can be also brought about by the front advancement itself, when the solidification has a dendritic character. During solidification the flow may hinder the assimilation of particles by the advancing front. For a given advancement rate we also have a critical velocity of fluid flow, above which the particles will be pushed away by the front, even if its rate exceeds the critical value. The critical value of fluid flow increases with the increasing size of particles, their density and coarseness and velocity of the advancing front face. The analyzed problem is complex, and its modeling requires actual cases, where the geometry of the system, type and magnitude of flow as well as surface properties of particles are specified.

During continuous casting of metal, the vertical solidification front is usually dendritic. For analytical purposes, this shape can be modeled by an artificial wall made of uniform spheres, as in Fig. 10.

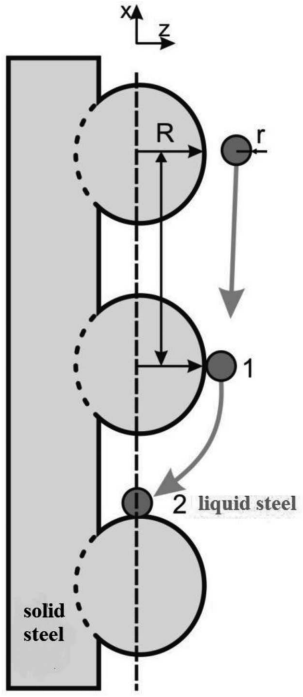

Fig. 10. Interaction of a spherical inclusion with crystallization front [11]

In the downward laminar flow of liquid steel the particles are engulfed after it passes the space between two neighboring spheres (site 2). If the components of the particle velocity were v_x and v_z (smooth front face), and u_x and u_z (coarse front face), then we have:

$$u_x = v_x \tag{23}$$

$$u_z = f \cdot v_z \tag{24}$$

Modification of the component velocity v_z by the coarse front is expressed by coefficient f. Having accounted for this factor we obtain a condition of particle assimilation after [10]:

$$\frac{R}{D-R} \leqslant \frac{f \cdot vz}{vx} \tag{25}$$

where:

D – distance between spheres in artificial rough front.

The distribution of fluid velocity along the direction can be approximated as:

$$V_H = 2V_0 \cdot \left(1 - \frac{(H-z)^2}{H^2}\right) \tag{26}$$

where:

H – distance between the particle and vertical solidification front [m],

z – horizontal coordinate.

The velocity of a particle moving downward can be calculated from the equation:

$$v_x = (v_0 + 2V_0) \cdot \left(1 - \frac{(H-z)^2}{H^2}\right) \tag{27}$$

v_0 – velocity of a particle in reference to the velocity of steel [m/s]

V_0 – average velocity of fluid (steel) flow downwards [m/s].

Velocity of particle v_0 in relation to liquid equals to:

$$v_0 = \frac{2r^2 \cdot g}{9\mu} \cdot \left(\rho_p - \rho_m\right) \tag{28}$$

The component of particle's velocity in a direction z can be calculated from the Saffman force dependence (20). The velocity gradient in the vicinity of the solidification front can be approximated by the following equation:

$$S = \frac{4 \cdot V_0}{H} \tag{29}$$

S – local gradient of fluid's velocity [m/s],

H – distance of a particle from vertical solidification front [m].

The velocity of a particle in reference to fluid can be determined from dependences (26) and (27):

$$u_p = v_0 \cdot \left(1 - \frac{(H-z)^2}{H^2}\right) \tag{30}$$

Hence the Saffman force equals to:

$$F_S = 6.46 \cdot \mu \cdot r^2 \cdot \left(\frac{4 \cdot V_0}{H \cdot \nu}\right) \cdot v_0 \cdot \left(1 - \frac{(H-z)^2}{H^2}\right) \tag{31}$$

This force is in equilibrium with the drag F_d. Having assumed $\theta = 1$ and $F_s = F_d$ we obtain:

$$\frac{R}{D-R} \leqslant 0.68 \cdot f \cdot r \cdot \sqrt{\frac{V_0}{H \cdot \nu}} \cdot \frac{r^2 \cdot \left(\rho_p - \rho_m\right) \cdot g}{r^2 \cdot \left(\rho_p - \rho_m\right) \cdot g + 9 \cdot \mu \cdot V_0} \tag{32}$$

Generally, the flow of fluid strongly affects the interaction of inclusions and the solidification front. The velocity of flow which is critical for given front parameters totally blocks the engulfment of particles. Higher critical velocities are needed for bigger and denser particles, and also for higher crystallization rates and for coarser surfaces. On the other hand, in the turbulent flow conditions, the component velocity of some particles towards the advancing solidification front is higher, therefore can be assimilated more readily. Coefficient f in equation (25) signifies that also turbulent flow takes place in the metal flow.

9. Calculation of velocity of non-metallic particle v_0 and velocity of particle vs. fluid u_p

The velocity of non-metallic particle v_0 and velocity of particle vs. fluid u_p were calculated on the basis of above presented equations (28) and (30). The following assumptions were made:

ρ_m – density of metal (steel) 7000 [kg/m^3],ρ_p – density of inclusion (Al_2O_3) 3990 [kg/m^3],

r – radius of non-metallic particle 0.00001-0.0001[m], H – distance of a non-metallic particle from the vertical solidification front 0.000001 [m], z – horizontal coordinate, z_1 = 0.00001 [m], z_2 = 0.00005 [m], z_3 = 0.0001 [m].

Results of calculations are presented in Figures 11 and 12.

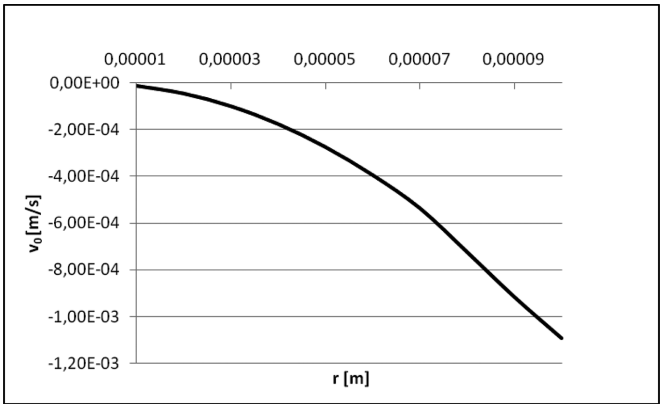

Fig. 11. Results of calculations of velocity of a non-metallic particle as a function of its radius

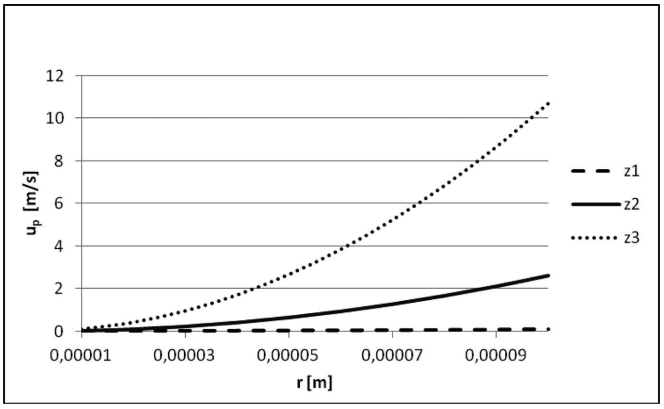

Fig. 12. Results of calculations of velocity of a non-metallic particle as a function of its radius and coordinate z

The velocity of a particle increases with the growth of its radius, which means that bigger inclusions leave the steel faster than their smaller counterparts. The obtained results suggest that the velocity of a non-metallic particle u_p in reference to liquid steel increases with its growing size, and this trend tendency is maintained for various locations of z; at higher values of z (z_3), the velocity u_p is higher.

10. Conclusion

Calculations for single particle near vertically advancing crystallization front show a conclusion that bigger inclusions are repelled by the front and accumulate in the central part of the ingot, whereas their smaller counterparts are distributed in the ingot evenly. The values of the surface tension σ_{s-l} and σ_{p-l} (variant 2) result in an increase of the repulsive force acting on the inclusions. On the other hand, the increase of the frictional force is also influenced by the increasing size of the particle and the rate at which the solidification front advances. Calculations of the drag force F_d force for a non-metallic particle in the vicinity of a vertical front advancing horizontally for variants, determine the influence of radius of an inclusion on force F_d. The F_d force values increase with the increasing radius of the inclusion particle and with the velocity of the advancing solidification front. The frictional force mainly acts on particles in the close vicinity of the solidification front. Calculation of velocity of non-metallic particle v_0 and fluid u_p show, that the velocity of a particle increases with the growth of its radius, which means that bigger inclusions leave the steel faster than their smaller counterparts.

Acknowledgements

This work was sponsored by Ministry of Science at the statute work at AGH Universityof Science and Technology (contract 11.11.170.318).

REFERENCES

[1] S. Kimura, Y. Nabeshima, K. Nakajima, S. Mizoguchi, Behavior of Nonmetallic Inclusions in Front of the Solid – Liquid Interface in Low Carbon Steel, Met. Trans.B **31**, B (2000).

[2] E. Fraś, E. Olejnik, Interaction Between Solidification Front and Alien Phase Particles, Archiv. Metall. Mat. **53** (3), 695-702 (2008).

[3] S. Omenyi, A.W. Neumann, Thermodynamic Aspects of Particle Engulfment by Solidifying Melts. J.Appl.Phys. **47**, 9 (1976).

[4] D.M. Stefanescu, R.V. Phalnikar, H. Pang, S. Ahuja, B.K. Dhindaw, A Coupled Force Field – Thermal Field Analytical Model for the Evaluation of the Critical Velocity for Particle Engulfment, ISIJ Int. **35**, 6 (1995).

[5] D. Sangguan, S. Ahuja, D.M. Stefanescu, An Analytical Model for the Interaction Between an Insoluble Particle and an Advancing Solid/Liquid Interface, Met. Trans. A, **23A** (1992).

[6] J. Pötschke, V. Rogge, On the Behaviour of Foreign Particles at Advancing Solid – Liquid Interface, J. Crystal Growth **94**, 726 (1989).

[7] D.M. Stefanescu, B.K. Dhindaw, S.A. Kacar, A. Moitra, Behavior of Ceramic Particles at the Solid – Liquid Metal Interface in Metal Matrix Composites, Met. Trans. A. **19A** (1988).

[8] Q. Han, J. Hunt, Redistribution of Particles during Solidification, ISIJ Int., 35 (1995).

[9] P.G. Saffman, The Lift on Small Sphere in a Slow Shear Flow, J. Fluid mech., 22 (1965).

[10] K. Mukai, M. Zeze, Motion of Fine Particles under Interfacial Tension Gradient in Relation to Continuous Casting Process, Steel Research **74**, 3 (2003).

[11] D. Kalisz, Thermodynamic Characteristic Formation of Non-Metallic Phase in the Liquid Steel, Krakow 2013.

[12] H. Shibata, H. Yin, S. Yoshinaga, T. Emi, M. Suzuki, In-situ Observation of Engulfment and Pushing of

Nonmetallic Inclusions in Steel Melt by Advancing Melt/Solid Interface, ISIJ Int. 38 (1998).

[13] S. Sen, B.K. Dhindaw, D.M. Stefanescu, A. Catalina, P.A. Curreri, Melt Convection Effects on the Critical Velocity of Particle Engulfment, J. Crystal Growth **173** (1997).

[14] J. Wypartowicz, D. Podorska, Interaction of Non-Metallic Inclusions in Steel with Advancing Solidification Front, Hutnik Wiadomości Hutnicze, 72 (2005).

[15] D. Podorska, J. Wypartowicz, Behaviour of Non-metallic Particles During Solidification of Silicon Steel, Conf. Metal 2004.

Received: 20 January 2014.